Determination of the Pulse Duration of an X-Ray Free Electron Laser Using Highly Resolved Single-Shot Spectra

Yuichi Inubushi,[1,*] Kensuke Tono,[2] Tadashi Togashi,[2] Takahiro Sato,[1] Takaki Hatsui,[1] Takashi Kameshima,[2] Kazuaki Togawa,[1] Toru Hara,[1] Takashi Tanaka,[1] Hitoshi Tanaka,[1] Tetsuya Ishikawa,[1] and Makina Yabashi[1]

[1]*RIKEN SPring-8 Center, Kouto 1-1-1 Sayo, Hyogo 679-5148, Japan*

[2]*Japan Synchrotron Radiation Research Institute, Kouto 1-1-1, Sayo, Hyogo 679-5198, Japan*

(Received 30 May 2012; published 1 October 2012)

We determined the pulse duration of x-ray free electron laser light at 10 keV using highly resolved single-shot spectra, combined with an x-ray free electron laser simulation. Spectral profiles, which were measured with a spectrometer composed of an ultraprecisely figured elliptical mirror and an analyzer flat crystal of silicon (555), changed markedly when we varied the compression strength of the electron bunch. The analysis showed that the pulse durations were reduced from 31 to 4.5 fs for the strongest compression condition. The method, which is readily applicable to evaluate shorter pulse durations, provides a firm basis for the development of femtosecond to attosecond sciences in the x-ray region.

DOI: 10.1103/PhysRevLett.109.144801 PACS numbers: 41.60.Cr, 06.60.Jn, 07.85.Nc, 41.50.+h

Recently, x-ray free electron lasers (XFELs) [1], such as the Linac Coherent Light Source [2] and SPring-8 Angstrom Compact free electron Laser (SACLA) [3], have successfully generated brilliant, femtosecond x-ray pulses, achieving an ultrahigh resolving power in both space and time that opens new frontiers in atomic physics [4,5] and optics [6], and the structural analysis of biological nanoparticles [7,8]. One of the key features of XFEL light enabling these new applications is an ultrafast pulse duration below 100 femtoseconds. Characterization of the temporal profile is crucially important for understanding and analyzing these new phenomena [9]. In the visible and infrared regions, correlation techniques based on nonlinear optical processes have been routinely utilized for evaluating ultrafast optical pulses [10], although they have not been extended to the x-ray regions.

Our approach described in this Letter is more "universal," being applicable to the whole wavelength region including the vacuum ultraviolet [11], soft x-ray regions [12,13], and hard x-ray regions, which utilizes the basic relationship of the Fourier transform between the temporal domain and the frequency domain [14]; microstructures in the frequency domain relate with macrostructures in the temporal domain. More specifically, the spike widths in the energy spectra become larger for shorter pulse durations, and vice versa. Guided by this principle, with the help of XFEL simulations, we performed measurements of spectra and applied them to determine the pulse durations of XFEL light. A notable advantage of this method is an increase of feasibility toward *shorter* pulse durations due to the relaxed requirement of the spectral resolution. An excellent resolution of $\sim$10 meV with a spectral range of a few eV, however, is still needed to cover a wide range of pulse durations from one femtosecond up to a subpicosecond region. Another essential requirement is to perform single-shot detection, because shot-to-shot changes of the spectra, which originate from the stochastic nature of the self-amplified spontaneous emission (SASE) [15–17] scheme, smear out the spike structures when we accumulate the spectra in multiple shots. We note that a measurement of speckle contrast was applied to estimate the pulse duration of hard x-ray FEL pulses, although the broader spectral resolutions, compared with the spike widths of SASE-FEL, provide limited information [18].

Our experiment was conducted at BL3 of SACLA [3]. The SACLA main accelerator boosted the electron-beam

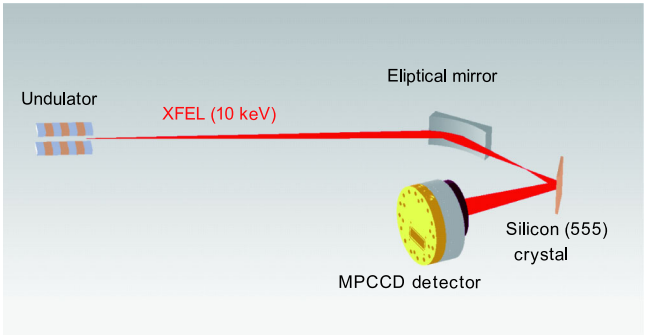

FIG. 1 (color online). Schematic configuration of the spectrometer. The spectrometer consists of an ultraprecisely figured elliptical mirror, an analyzer silicon (555) crystal, and a MPCCD detector. The elliptical mirror was coated with rhodium. The grazing incident angle was 2.7 mrad, the length of the mirror was 100 mm, and the focal length was 85 mm. The mirror enlarged the divergence angle of the x-ray beam to 2.5 mrad along the dispersion direction of the spectrometer. The silicon crystal with a Bragg angle of 81.3 deg for 10-keV x rays was located at 0.6 m from the elliptical mirror. The MPCCD detector, with a pixel size of 50×50 μm^2, was set at 3.6 m from the silicon crystal. These components are set in the horizontal plane (π polarization). The resultant spectral resolution and range were 20 meV and 4.2 eV, respectively.

energy up to 7 GeV. During the acceleration, a three-stage bunch compression system increased the peak current from 1 A to the kiloamperes level [19]. The in-vacuum, short-period undulator generated XFEL light with a photon energy of $E = 10$ keV and a spectral bandwidth of 40 eV full width at half maximum (FWHM). For performing a single-shot, high-resolution measurement of the spectra, we developed a spectrometer [20] consisting of an ultraprecisely figured elliptical mirror, an analyzer flat crystal of silicon (555), and a multiport charge coupled device (MPCCD) detector, as shown in Fig. 1. The spectral range $\Delta\varepsilon$ of a dispersive spectrometer using Bragg reflection is described by

$$\Delta\varepsilon = \frac{\Delta\theta\,\varepsilon}{\tan(\theta_B)}. \quad (1)$$

Here, θ_B is the Bragg angle, which is 81.3 deg for 10-keV x rays. ε is the photon energy. $\Delta\theta$ is the divergence angle of the x-ray beam. Although $\Delta\theta$ for XFEL radiation (~ 2 μrad) was too small to obtain sufficient spectral range, the elliptical mirror was utilized to enlarge the divergence angle to 2.5 mrad. The resultant spectral range was 4.2 eV. The spectral resolution $d\varepsilon/\varepsilon$ is described by

$$\frac{d\varepsilon}{\varepsilon} = \frac{\sqrt{\sigma^2 + L^2\omega^2}}{L\tan(\theta_B)}. \quad (2)$$

Here, σ is an x-ray source size corresponding to the focal spot size of 56 nm calculated using the Fresnel diffraction integral, L is the distance from the source to detector (4.2 m), and ω is the FWHM of the Darwin curve for the Bragg reflection for π polarization. The spectral resolution was measured to be 14 meV, which agreed with that given by Eq. (2), using monochromatic incident x rays. These properties enabled us to evaluate pulse durations from a femtosecond to subpicosecond region.

First, we show a typical single-shot spectrum in Fig. 2(a), which was measured at a normal bunch compression (condition 1). We found that the spike features could be completely resolved with the spectrometer. Next, we increased the bunch compression strength and reduced

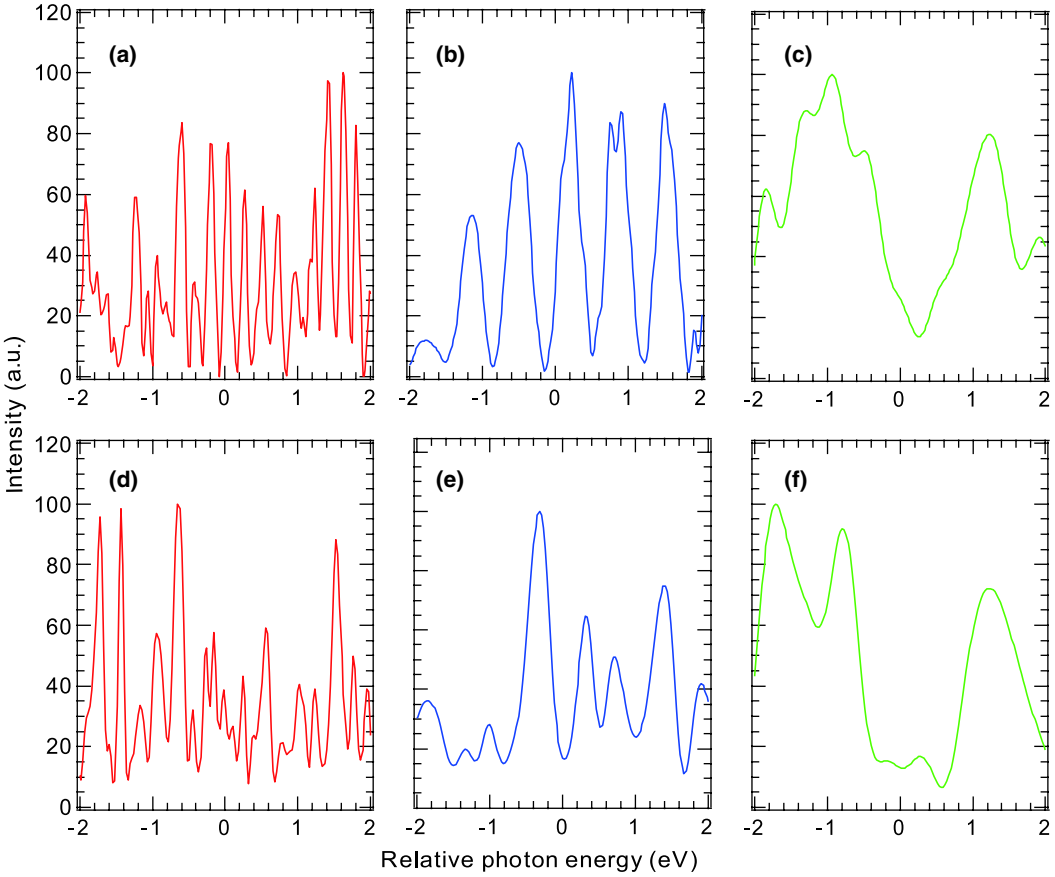

FIG. 2 (color online). Measured single-shot spectra of XFEL for (a) compression condition 1, (b) compression condition 2, and (c) compression condition 3. The horizontal axis indicates relative photon energy from the central value of $E = 9997$ eV. The weighted-average width δ of the spikes was determined to be (a) $\delta_1 = 110$ meV, (b) $\delta_2 = 290$ meV, and (c) $\delta_3 = 600$ meV in FWHM. (d)–(f) Simulated spectra with the average spike widths that are the same as those in (a)–(c), respectively. In the simulation, we used the energy chirps of the electron-beam $(\Delta E/E)/dt = (d)2 \times 10^{-5}$ fs^{-1}, (e) 4×10^{-5} fs^{-1}, and (f) 8×10^{-5} fs^{-1} for conditions 1, 2, and 3, respectively.

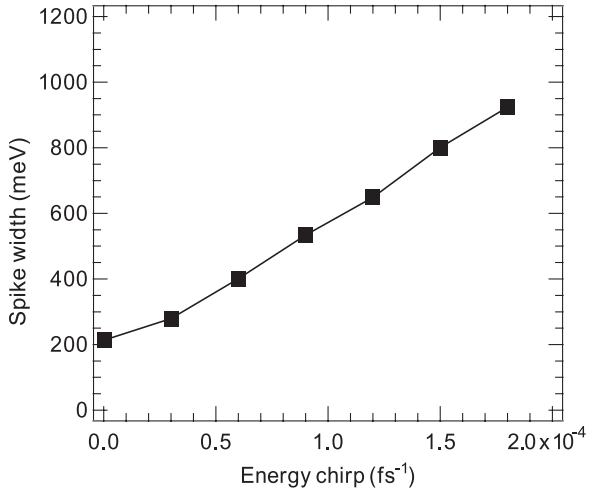

FIG. 3. Dependence of the simulated spike width on electron energy chirp. The bunch duration of the electron beam was fixed at 19 fs. The spike widths were obtained from the simulated spectra by fitting multiple Gaussian distributions, which is the same method as applied to the experimental data analysis.

the bunch duration (condition 2). An example of the measured spectra is presented in Fig. 2(b), which exhibits a broadening of the spike width. As we further increased the compression strength (condition 3), the observed spike widths became significantly broader, as seen in Fig. 2(c). For quantifying the spike widths, we employed the weighted-average widths δ of the spikes, which were determined by fitting the spectra with multiple Gaussian distributions. The widths obtained were $\delta_1 = 110$ meV, $\delta_2 = 290$ meV, and $\delta_3 = 600$ meV in FWHM for conditions 1, 2, and 3, respectively.

As a preliminary estimation, we performed a Fourier transform of the spike by assuming a Gaussian distribution of the width δ_i ($i = 1, 2, 3$) with a constant phase distribution. The product of pulse duration (FWHM) and spectral width (FWHM) is 1.8 fs eV in this case. The corresponding pulse durations were $\Delta T_{G1} = 16$ fs, $\Delta T_{G2} = 6.2$ fs, and $\Delta T_{G3} = 3.0$ fs for conditions 1, 2, and 3, respectively. However, this simple approach could result in substantial error because we neglected to account for the influence of the energy chirp of the electron beam, which can broaden the spike width. This situation is presented in Fig. 3, which was derived from a FEL simulation code, SIMPLEX [21].

For a more reliable and quantitative analysis, we simulated the spectra using SIMPLEX, and compared them with the experimental results. Among properties of the electron beam, two parameters were particularly important in this analysis: the bunch duration and the energy chirp. The former was treated as the only unknown parameter and a variable in the simulation. The latter parameter was dominated by the resistive-wall wakefield along the magnetic arrays of the in-vacuum undulator used for SACLA. Quantitatively, the energy chirps were evaluated to be 2×10^{-5} fs^{-1}, 4×10^{-5} fs^{-1}, and 8×10^{-5} fs^{-1} for conditions 1, 2, and 3, respectively, using the bunch-current profiles measured with a rf deflecting cavity [22] and a model function of the resistive-wall wakefield [23] of the undulator magnets. Naturally, the energy chirp increased for the stronger compression conditions with a higher peak current. We note that the validity of the model function was confirmed experimentally by evaluating the loss of the electron-beam energy through the measurement of the wavelength shift of the spontaneous radiation of the undulator.

The simulated spectra, which had average spike widths δ equivalent to the experimental values in Figs. 2(a)–2(c), are shown in Figs. 2(d)–2(f), respectively. The temporal profiles that correspond to these spectra are shown in Figs. 4(a)–4(c). We observed a significant change in the profiles for the different bunch compression conditions. The pulse durations, which are given by the envelopes of the profiles, were determined to be $\Delta T_1 = 31$ fs and

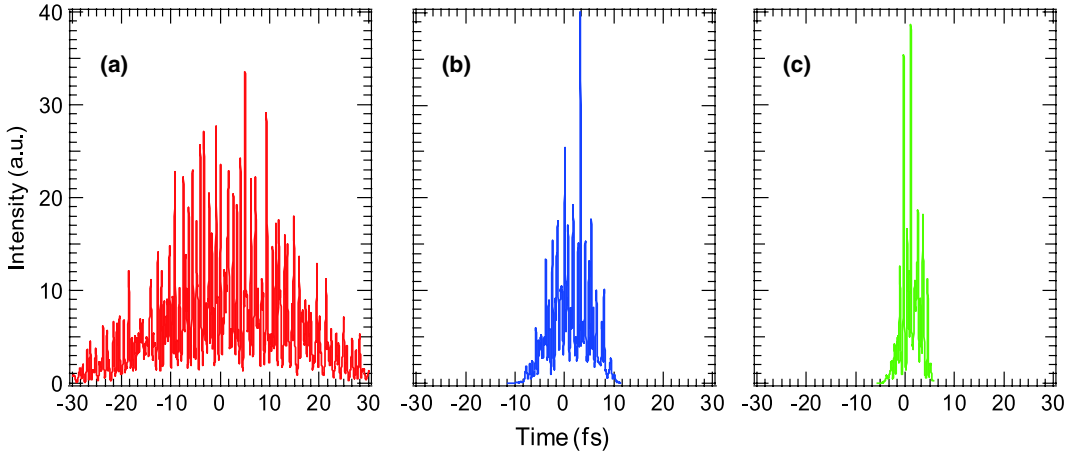

FIG. 4 (color online). (a)–(c) Simulated temporal profiles of XFEL pulses that correspond to the energy spectra in Figs. 2(d)–2(f). The pulse durations were (a) $\Delta T_1 = 31$ fs, (b) $\Delta T_2 = 8.9$ fs, and (c) $\Delta T_3 = 4.5$ fs.

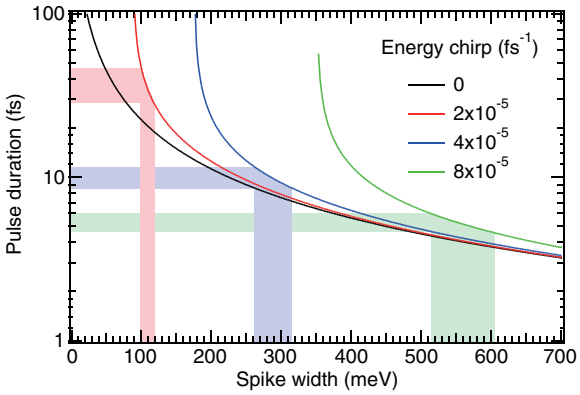

FIG. 5 (color online). XFEL pulse duration as functions of spike widths for several electron energy chirps. Experimental results are shown by the red region (condition 1), the blue region (2), and the green region (3). The pulse durations were determined to be 34^{+13}_{-7} fs, $9.7^{+2.3}_{-1.2}$ fs, and $5.1^{+0.8}_{-0.5}$ fs, respectively.

$\Delta T_2 = 8.9$ fs for conditions 1 and 2, respectively. For condition 3, the strongest compression, the pulse duration was reduced to $\Delta T_3 = 4.5$ fs. The pulse durations ΔT_i determined from the SIMPLEX simulations that correctly accounted for the chirp effect were considerably larger than ΔT_{Gi}, which was obtained with the simple Fourier transform for each of the conditions.

We applied this method to the statistical evaluation of the pulse duration. A similar analysis of a number of the measured, single-shot spectra allowed us to determine the mean and the rms deviations for the average spike widths to be $\bar{\delta}_1 = 110 \pm 9.8$ meV, $\bar{\delta}_2 = 290 \pm 28$ meV, and $\bar{\delta}_3 = 560 \pm 44$ meV. These values were converted to pulse durations of 34^{+13}_{-7} fs, $9.7^{+2.3}_{-1.2}$ fs, and $5.1^{+0.8}_{-0.5}$ fs, respectively, using the relationship among the spike width, the energy chirp, and the pulse duration given by the SIMPLEX simulation, shown in Fig. 5. The deviation is reasonably small for condition , although it becomes larger for condition 1 in spite of the similar deviations of the average spike widths ($< 10\%$). This result is explained by the dependences shown in Fig. 5. That is, the pulse duration for the longer-pulse condition (1) has a higher sensitivity to the change of the spike width. Since the sensitivity becomes much more moderate for condition 3, we can conclude that this method is more accurate and reliable for evaluating pulse durations below 10 fs.

Finally we discuss a future perspective. Although the present SASE scheme is able to produce multimode x-ray pulses with durations ranging from a few femtoseconds to subpicosecond, new schemes, such as the narrow-slit slicing technique and an enhanced SASE, have been proposed for generating attosecond x-ray pulses [24,25]. The method we have presented is readily applicable for these cases, especially towards shorter pulse durations. For example, utilization of an analyzer crystal of rubidium acid phthalates (001) would provide a wider spectral range of 590 eV, which is applicable to the characterization of 10-as pulses. This configuration would certainly provide a valuable tool for advancing x-ray attosecond sciences.

*inubushi@spring8.or.jp

[1] B. W. J. McNeil and N. R. Thompson, Nature Photon. **4**, 814 (2010).
[2] P. Emma *et al.*, Nature Photon. **4**, 641 (2010).
[3] T. Ishikawa, Nature Photon. **6**, 540 (2012).
[4] L. Young *et al.*, Nature (London) **466**, 56 (2010).
[5] S. M. Vinko *et al.*, Nature (London) **482**, 59 (2012).
[6] N. Rohringer *et al.*, Nature (London) **481**, 488 (2012).
[7] H. N. Chapman *et al.*, Nature (London) **470**, 73 (2011).
[8] M. M. Seibert *et al.*, Nature (London) **470**, 78 (2011).
[9] A. Barty *et al.*, Nature Photon. **6**, 35 (2012).
[10] E. P. Ippen and C. V. Shank, Appl. Phys. Lett. **27**, 488 (1975).
[11] V. Ayvazyan *et al.*, Phys. Rev. Lett. **88**, 104802 (2002).
[12] A. A. Lutman, Y. Ding, Y. Feng, Z. Huang, M. Messerschmidt, J. Wu, and J. Krzywinski, Phys. Rev. ST Accel. Beams **15**, 030705 (2012).
[13] C. Behrens, N. Gerasimova, Ch. Gerth, B. Schmidt, E. A. Schneidmiller, S. Serkez, S. Wesch, and M. V. Yurkov, Phys. Rev. ST Accel. Beams **15**, 030707 (2012).
[14] J. W. Goodman, *Statistical Optics* (Wiley, New York, 1985).
[15] R. Bonifacio, C. Pellegrini, and L. M. Narducci, Opt. Commun. **50**, 373 (1984).
[16] A. M. Kondratenko and E. L. Saldin, Part. Accel. **10**, 207 (1980).
[17] E. L. Saldin, E. A. Schneidmiller, and M. V. Yurkov, New J. Phys. **12**, 035010 (2010).
[18] C. Gutt *et al.*, Phys. Rev. Lett. **108**, 024801 (2012).
[19] K. Togawa, T. Hara, and H. Tanaka, Phys. Rev. ST Accel. Beams **12**, 080706 (2009).
[20] M. Yabashi, J. B. Hastings, M. S. Zolotorev, H. Mimura, H. Yumoto, S. Matsuyama, K. Yamauchi, and T. Ishikawa, Phys. Rev. Lett. **97**, 084802 (2006).
[21] T. Tanaka, *Proceedings of the 26th International FEL Conference and 11th FEL users Workshop*, (JACoW, Geneva, 2004) p. 435; see also http://radiant.harima.riken.go.jp/simplex.
[22] H. Ego, H. Maesaka, Y. Otake, T. Sakurai, T. Hashirano, and S. Miura, *Proceedings of IPAC2011*, 1221 (JACoW, Geneva, 2011).
[23] K. L. F. Bane and G. Stupakov, Report No. SLAC-PUB-10707, 2004.
[24] A. A. Zholents and W. M. Fawley, Phys. Rev. Lett. **92**, 224801 (2004).
[25] P. Emma, K. Bane, M. Cornacchia, Z. Huang, H. Schlarb, G. Stupakov, and D. Walz, Phys. Rev. Lett. **92**, 074801 (2004).